



Published in final edited form as:

Environ Sci Technol. 2017 December 05; 51(23): 13714–13722. doi:10.1021/acs.est.7b04220.

Metabolism and Photolysis of 2,4-Dinitroanisole in *Arabidopsis*

Hunter W. Schroer[†], Xueshu Li[‡], Hans-Joachim Lehmler[‡], and Craig L. Just^{*†}

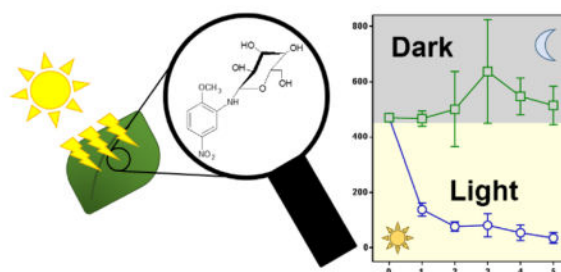
[†]Civil & Environmental Engineering, The University of Iowa, Iowa City, Iowa 52242, United States

[‡]Occupational & Environmental Health, The University of Iowa, Iowa City, Iowa 52246, United States

Abstract

New insensitive munitions explosives, including 2,4-dinitroanisole (DNAN), are replacing traditional explosive compounds to protect soldiers and simplify transport logistics. Despite the occupational safety benefits of these new explosives, feasible strategies for cleaning up DNAN from soil and water have not been developed. Here, we evaluate the metabolism of DNAN by the model plant *Arabidopsis* to determine whether phytoremediation can be used to clean-up contaminated sites. Furthermore, we evaluate the role of photodegradation of DNAN and its plant metabolites within *Arabidopsis* leaves to determine the potential impact of photolysis on the phytoremediation of contaminants. When exposed to DNAN for three days, *Arabidopsis* took up and metabolized 67% of the DNAN in hydroponic solution. We used high resolution and tandem mass spectrometry in combination with stable-isotope labeled DNAN to confirm ten phase II DNAN metabolites in *Arabidopsis*. The plants separately reduced both the *para*- and *ortho*-nitro groups and produced glycosylated products that accumulated within plant tissues. Both DNAN and a glycosylated metabolite were subsequently photolyzed within leaf tissue under simulated sunlight, and [¹⁵N₂]DNAN yielded ¹⁵NO₂ in leaves. Therefore, photolysis inside leaves may be an important, yet under-explored, phytoremediation mechanism.

Graphical Abstract



INTRODUCTION

Explosive compounds contaminate millions of land acres globally, primarily through releases at military training facilities (e.g., as unexploded ordnance) and at production and

* craig-just@uiowa.edu. Phone: 319-335-5051. Fax: 319-335-5660.

disposal facilities.^{1, 2} Utilization of the most common explosives, 2,4,6-trinitrotoluene (TNT) and hexahydro-1,3,5-trinitro-1,3,5-triazine (RDX), is projected to decrease as insensitive munitions gain favor in new melt cast explosives formulations.^{1, 3} For example, the formulation “IMX-101,” comprised of 2,4-dinitroanisole (DNAN), nitrotriazolone, and nitroguanidine, provides a similar explosive force to TNT, but with a decreased sensitivity to shocks that can trigger unintended detonations.⁴ DNAN ($S_w = 276 \text{ mg L}^{-1}$), used in at least six modern explosives formulations, is considerably more water-soluble than TNT and RDX ($S_w = 100$ and 60 mg L^{-1} , respectively), which elevates concern for groundwater contamination.⁴⁻⁷ DNAN is also less sorptive than TNT and RDX, which makes contaminant plume migration more likely while rendering site cleanup more difficult and expensive.³ Remediation of explosives is typically achieved by costly *ex situ* methods, such as pump and treat or incineration.⁸ Alternatively, *in situ* bioremediation is potentially less expensive, and biotic systems have been used to remediate legacy explosives such as TNT and RDX.⁸⁻¹⁸

One biotic remediation approach, phytoremediation, is the use of plants to metabolize or even sequester harmful chemicals irreversibly into biomass.¹⁹ When exposed to organic contaminants, plants may metabolize the compound following the conceptual framework called the “green liver” model. The green liver model posits that xenobiotics are functionalized in phase I (e.g., hydroxylation, nitro-reduction, demethylation). In phase II metabolism, plants conjugate large, water-soluble moieties, such as glucose onto the new functional group. Plants can also perform phase II conjugation without phase I functionalization if the original compound contains a sufficiently reactive moiety.^{9, 19, 20} The phase II metabolites are subject to further degradation or permanent sequestration to cell walls or vacuoles in phase III of metabolism, which make plants a promising option for long-term contaminant remediation.^{9, 11, 12, 19, 21} Specifically with regards to explosives, plants can functionalize TNT via nitro group reductions to hydroxylamines and amines prior to conjugation with glutathione and sugars – precursors to non-extractable, covalently-bound TNT residues, containing and detoxifying the explosives.^{9, 11, 12, 22, 23} Additionally, plants facilitate the degradation of photo-labile explosives such as RDX through uptake, translocation to leaves, and subsequent photolysis. In one study, sunlight exposure degraded RDX within reed canary grass leaves, while in the absence of sunlight, the grass did not metabolize RDX.²⁴ In another study, both light and *Populus* tissue culture cells were required for RDX mineralization, indicating a light-induced transformation inside the plant cells.²⁵ Despite these promising results, the role of sunlight in phytoremediation (i.e., photophotolysis) has largely been overlooked for other compounds.²⁶

Although photolysis and metabolism in plants has been demonstrated for RDX and TNT, respectively, there is little data available on plant metabolism of DNAN and the potential to clean up DNAN-contaminated sites with phytoremediation. A limited number of studies have investigated DNAN chemical and biochemical transformations, soil binding behavior, and ecotoxicity.^{1, 3, 27-32} One study reported DNAN in grass shoots and roots, but no mass balance was reported and no transformation products were measured.³³ Another study observed DNAN metabolism in ryegrass where DNAN was reduced to 2-amino-4-nitroanisole (2-ANAN) and further conjugated to unknown, acid-hydrolysable products, possibly sugars.¹ However, it remains unknown whether plant metabolites of *any*

xenobiotics can undergo photolysis inside photosynthetic tissues, potentially altering the phytoremediation process. We are unaware of any previous reports of DNAN, or DNAN metabolite, photolysis inside plant tissues despite knowledge that DNAN, and a model plant metabolite of DNAN (4-nitrophenyl- β -D-glucopyranoside), are photolyzed in aqueous solution.^{3, 34} Here, we report DNAN metabolism and photolysis within the model plant *Arabidopsis*.

MATERIALS & METHODS

Chemicals—All reagents and standards were used as received with sources and purities listed in the supporting information (SI). [¹³C₆]DNAN (>99%) and [¹⁵N₂]DNAN (>99%) were synthesized as previously described.²⁹ Liquid chromatography solvents (Optima grade) were purchased from Fisher Scientific (Waltham, MA, USA).

Experimental Design

Plant growth conditions—*Arabidopsis thaliana* (Col-0) was studied due to its extensive use and characterization in basic research and to compare with previous studies on *Arabidopsis* metabolism of explosives.^{9, 22, 35, 36} Before exposure to DNAN, *Arabidopsis thaliana* (Col-0) seeds were sterilized using a bleach solution and stratified for 1–5 days in sterilized deionized (DI) water at 4 °C.³⁵ After stratification, seeds or seedlings were placed into Magenta boxes (Magenta LLC., Lockport, IL, USA) containing 25 mL of filter-sterilized (0.2 μ m, cellulose nitrate, Nalgene, Rochester, NY, USA) Murashige and Skoog (MS) basal medium³⁵ (see SI for recipe). The boxes were incubated in a growth chamber (Percival Scientific, Perry, IA, USA) with a diurnal cycle of 16 hours of light (23 °C) and 8 hours of dark (21 °C) at 50% relative humidity. At the basal medium surface, the light intensity was $140 \pm 19 \mu\text{mol photons m}^{-2} \text{s}^{-1}$ (photosynthetically active range) as measured three times per week by a quantum light sensor (LI-COR, Lincoln, NE, USA).

DNAN and metabolite mass balance—To determine a DNAN mass balance in plant media and tissues, hydroponic cultures of *Arabidopsis* were sacrificed every 12 hours over three days of DNAN exposure. Plants (n = 25 seeds per box) were exposed to DNAN after 14 days of seed germination and growth, at which point the medium in each Magenta box (n = 18) was replaced with fresh, sterile medium (25 mL) spiked with 125 nmoles DNAN (dissolved in 250 μ L methanol, 1% v/v) to achieve a nominal concentration of 5 μ M (1 mg/L). This relatively high DNAN concentration was selected to facilitate metabolite identification after preliminary uptake experiments indicated no visible physiological plant effects at 5 (Figure S1). Every 12 hours, randomly selected, whole Magenta boxes were sacrificially harvested in triplicate. Control boxes, containing MS medium and DNAN, but no plants, were simultaneously harvested in duplicate. Hydroponic media was analyzed by mass spectrometry and plant tissues were extracted as described below.

Metabolite identification experiments—Metabolites of DNAN were identified using an untargeted metabolomics approach, enhanced by stable-isotope labeled DNAN. Three exposure conditions (n = 12 boxes, 25 seeds per box) were conducted simultaneously: 1) non-labeled DNAN with [¹³C₆]DNAN (31 nmoles each), 2) non-labeled DNAN with

[¹⁵N₂]DNAN (31 nmoles each), and 3) no added DNAN. After 14 days of germination and growth, the MS medium was replaced with fresh medium (25 mL) containing non-labeled DNAN and labeled DNAN (dissolved in methanol) as above to a nominal concentration of 2.5 μM. The equivalent volume of methanol (250 μL, 1% v/v) was added to the no-DNAN controls. After 48 hours, quadruplicate boxes of each treatment type were harvested, extracted, and analyzed by liquid chromatography high-resolution mass spectrometry with data processing via metabolomics software as described below.

Photolysis experiments—Irradiation experiments used an Atlas Suntest CPS+ solar simulator (Atlas Material Testing Technology, Mount Prospect, IL, USA) with a xenon lamp and an Atlas UV Suntest filter to simulate the emission spectrum of natural sunlight at an irradiance of 750 W/m² (Figure S2) and the irradiation chamber was cooled to 19.9 ± 0.6 °C during experiments using a portable air conditioning unit. To determine if DNAN and its metabolites were photolyzed inside leaves, we exposed *Arabidopsis* plants to DNAN and then exposed the leaves to simulated sunlight. *Arabidopsis* seeds were sterilized and stratified in the same manner as described above. Next, approximately 1000 seeds were placed into MS medium (150 mL) in a foam-stoppered, 500 mL flask. The flask was incubated in the growth chamber on a shaker table (120 rpm). After seven days, germinated seedlings were placed into Magenta boxes (n = 20 per box) with 25 mL of fresh MS medium. After seven days of additional growth, the seedlings were exposed to 5 μM [¹⁵N₂]DNAN in 25 mL of fresh MS medium. After 48 hours in the growth chamber, leaves were excised from roots, and the leaves from each Magenta box were divided into two groups. The “irradiation treatment” leaves were placed into cork-stoppered quartz tubes positioned at 30° from horizontal within the solar simulator. The “non-irradiated control” leaves were placed into sealed 2 mL vials wrapped in aluminum foil before positioning inside the solar simulator. Each hour, triplicate sets of irradiated and non-irradiated leaves were removed from the solar simulator and the fresh weight was recorded before lyophilization. In a separate experiment to examine DNAN transformation products from solar irradiation of *Arabidopsis* leaves, 125 nmoles of DNAN was added to each box (n=10 boxes, 20 seedlings each) to a nominal concentration of 5 μM. After two days of DNAN exposure, excised leaves were divided into irradiated and non-irradiated groups. Leaves were either exposed to simulated sunlight or kept in the dark for three hours before freeze-drying, solvent extraction, analysis, and data processing.

Analytical Methods

Liquid chromatography and mass spectrometry—Quantitative mass spectrometry analyses were performed on a liquid chromatograph (Agilent model 1260, Santa Clara, CA, USA) and triple-quadrupole (LC-QQQ) mass spectrometer (Agilent model 6460) equipped with a Jet Stream electrospray ionization (ESI) source. Samples in the auto-sampler tray were maintained at 8 °C. DNAN and other metabolites were quantified in ESI negative (ESI⁻) and positive (ESI⁺) modes and verified with a second fragment ion using the mass transitions, analytical columns, and mobile phase conditions outlined in the SI, Table S2. DNAN was quantified using a six-standard, [¹³C₆]DNAN internal standard-normalized, external calibration curve run before each batch. Amino-nitroanisoles were quantified by an external calibration curve of the respective standards diluted from stock solutions, without

adjusting for the internal standard due to separate runs in different ionization modes from DNAN. Agilent MassHunter Quantitative Analysis software was used to fit a linear calibration curve. For quality control, three to four check standards from the calibration curve were analyzed per batch (25–75 samples) to ensure consistent detector response. A deionized (DI) water blank was run every five injections to ensure there was no sample carry-over contamination. Analyses requiring accurate mass data were performed by ultraperformance liquid chromatograph with a quadrupole time-of-flight (LC-QToF) mass spectrometer or an Orbitrap (LC-Orbitrap) mass spectrometer with specifics of instrumentation, columns, mobile phase gradients, and instrument parameters described in the SI.

Plant tissue extraction, metabolite hydrolysis, and nitrite derivitization—At each sampling time, plant tissue was removed from the medium and dabbed dry with a Kimwipe (Kimberly-Clark, Irving, TX, USA). The plant tissue was placed into a 2 mL vial (safe-lock, Eppendorf) and the fresh weight was recorded before freezing (−80 °C) and subsequent lyophilization (FreeZone 6, Labconco, Kansas City, MO, USA) for 13–16 hours. The dry weight (52–75 mg, mean: 69 mg dry weight for whole plants; 10–17 mg, mean: 13 mg for leaf fractions) of the freeze-dried tissue was recorded and a single stainless steel ball (5 mm) and 1 mL water:methanol (1:1) mixture were added to each vial. The vials were frozen (−80 °C), thawed, and homogenized by a mixer mill (Retsch, Haan, Germany) for 5 min at 30 Hz. The vials were then sonicated for 10 min, vortexed for 30 s and centrifuged at 13,000g for 10 min. Finally, the supernatant was removed and syringe-filtered (0.22 μm, PES, Chemglass Life Sciences, Vineland, NJ, USA). The tissue was extracted without the freeze-thaw step two additional times with 500 μL of water:methanol (1:1) and the supernatants were combined.³⁵ Samples for metabolite identification were extracted only once, with 1 mL of water:methanol (1:1) mixture. Reported concentrations of DNAN and metabolites were corrected for a 95.7 ± 0.6 % extraction efficiency (determined from spike recoveries on unexposed plant tissues after three extractions). An internal standard (250 nM [¹³C₆]DNAN final concentration) was added after extracts were diluted (with DI water) to fall within the calibrated range of the mass spectrometer. In a preliminary test for sorption of DNAN to Magenta boxes, we decanted DNAN-containing media from two boxes, rinsed the boxes with 1 mL of water:methanol (1:1), and analyzed this fraction for DNAN. This procedure resulted in negligible recovery of DNAN (< 0.1%), therefore, we concluded that DNAN sorption to the boxes was not important and did not repeat the procedure for each experiment.

For glycosylated metabolite analysis, tissue extracts were prepared as above and hydrolyzed with acid prior to analysis for released 2-ANAN by adding 30 μL of sample, 30 μL DI water, and 30 μL of 1.5N HCl to a 150 μL vial insert inside a 2 mL LC autosampler vial. The extracts were incubated at 45 °C for 5 min and analyzed immediately by LC-QQQ. Isotope-labeled nitrite was measured by LC-QQQ after derivitization with 2,3-diaminonaphthalene (DAN) using a method modified from Nussler, et al.³⁷ Briefly, 5 μL of leaf extract was diluted with 95 μL of DI water prior to derivitization with 50 μL of DAN (158 μM in 0.62 N HCl) and 50 μL of 1.5N HCl for 10 minutes at room temperature. To quench the reaction, 20 μL of 1N NaOH was added and the samples were incubated at 8 °C for at least 90 minutes

prior to analysis. Labeled nitrite in plant extracts was calibrated to derivitized standards with a known amount of spiked $^{15}\text{NO}_2$ in DI water and $1.1\ \mu\text{M}\ \text{NO}_2$ as a background concentration similar to plant extracts.

Unknown metabolite identification and statistical analysis—Full-scan LC-QToF data of whole plant extracts were collected for ten minutes, converted to netCDF format by Databridge software (Waters, Milford, MA, USA) and uploaded to XCMS Online³⁸ for an untargeted metabolomics approach to metabolite elucidation. This study examined compounds resulting from DNAN transformation as confirmed by stable-isotope labeled substrates, and, as such, was not a comprehensive metabolomics investigation. Three DNAN isotopologues (i.e., unlabeled DNAN, $^{13}\text{C}_6$ DNAN, and $^{15}\text{N}_2$ DNAN) were used to allow unambiguous identification of metabolites derived from DNAN and to provide orthogonal data sets. Full XCMS Online parameters are detailed in Table S3. Elemental formulas were assigned based on the averaged accurate mass of all biological replicates using Thermo Xcalibur software. Raw, time-series concentration data were compared for significant differences using a two-sided, matched-pairs Student's t-test ($\alpha = 0.05$, $p < 0.05$). Figures were produced and statistical analysis was conducted using GraphPad Prism 7.00 and PerkinElmer Chemdraw Prime 16.0.1.4.

RESULTS AND DISCUSSION

Arabidopsis takes up and metabolizes DNAN—To determine if *Arabidopsis* can take up and metabolize DNAN, plants were exposed to DNAN for three days in hydroponic medium under sterile conditions. Plants quickly took up DNAN from solution, with 67% of DNAN mass removed over 72 hours (Figure 1). In a no-plant control, some DNAN was transformed, presumably due to photolysis because DNAN is stable in solution in the dark, and DNAN was not sorbed to Magenta boxes.³ However, the DNAN concentration in planted media was significantly different from the controls ($p = 0.0005$, $n = 6$ pairs). *Arabidopsis* removed DNAN from the hydroponic medium with pseudo-first order kinetics ($k_{\text{obs}} = 0.33 \pm 0.03\ \text{d}^{-1}$). DNAN uptake by *Arabidopsis* is consistent with previous work where DNAN was detected in grass grown on soil amended with DNAN, as well as with other studies of plant metabolism of xenobiotics.^{1, 20, 33, 35, 36} Of the DNAN taken up from solution, a maximum of 13% was found within the plant tissues after 12 hours, suggesting that DNAN was extensively metabolized. We detected 2-ANAN and 4-amino-2-nitroanisole (4-ANAN) in plant tissue and media at low levels (Figure S3), indicating that *Arabidopsis* reduced both nitro groups. The *ortho* reduction product was present in 4–5 times the abundance of the *para* reduction product, consistent with other studies of DNAN transformation.^{3, 27, 28, 32} Acid hydrolysis of extracts increased the 2-ANAN concentration, suggesting a conjugated product similar to that found in ryegrass (Figure S4).¹

Despite –or as a result of– their immobile nature, plants have adapted diverse enzymes for detoxifying xenobiotic compounds.¹⁹ Indeed, *Arabidopsis* has over 60 genes encoding cytochrome P450 enzymes and metabolizes a variety of chemicals.²¹ For example, *Arabidopsis* quickly assimilates and metabolizes benzotriazole and 2-mercaptobenzothiazole in hydroponic media, while carrots and horseradish conjugate the antibacterial agent

triclosan.^{20, 35, 36, 39} *Arabidopsis* also takes up and transforms the structurally similar TNT.^{9, 22} While the detected phase I and phase II metabolites were not unexpected based on the green liver model and plant metabolism of TNT, the low mass balance of DNAN and phase I metabolites from LC-QQQ analysis indicated that further investigation was required to identify unknown DNAN metabolites.

Arabidopsis conjugates DNAN with sugars and glutathione—To detect DNAN transformation products, we utilized an untargeted metabolomics approach, which identified sugar conjugates M330, M568, M524, and M376 and glutathione conjugates M699 and M669 (Table 1, Figure 2). All discovered metabolites were confirmed using stable isotope-labeled DNAN, and the metabolites in Table 1 each contained all respective stable isotopes (see Tables S4 and S5 for labeled metabolites). DNAN metabolites contained all the original isotope labels, indicating that *Arabidopsis* did not mineralize the aromatic ring of DNAN, nor did the plants remove the original nitrogen atoms from DNAN. These sugar and glutathione conjugates are therefore consistent with the green liver model of plant metabolism.

DNAN metabolites M669 and M699 both contained multiple characteristic glutathione mass fragments in both ESI⁺ and ESI⁻ mode (Table 1). The observed mass fragments indicate that the glutathionyl group was conjugated to an aromatic or benzylic group.⁴¹ In addition, the molecular masses of metabolites M669 and M699 differ by an average m/z of 30.0105 corresponding to a neutral loss of CH₂O (m/z 30.0106). We hypothesize that M699 results from direct conjugation to the aromatic ring at a previously unsubstituted position, and that M669 results from a sulfhydryl substitution for the DNAN methoxy group (Figure 2A). Glutathione conjugation is a well-known detoxification process for electrophilic xenobiotics, including nitro-aromatics and resulting hydroxylamine reduction products.⁹ Furthermore, glutathione conjugates of DNAN are consistent with a specific pathway that *Arabidopsis* utilizes to detoxify TNT *via* glutathione transferases (GSTs). Importantly, an isolated GST catalyzed denitration of TNT, which would increase bioavailability and significantly decrease the toxicity of the TNT metabolite.⁹ However, our observed products retained both original nitrogen atoms as confirmed with ¹⁵N-labeled DNAN.

The identification of M483 and M513 (Table 1) suggests that the glutathione metabolites were further degraded to S-cysteinyl conjugates. This process has been described for glutathione conjugates of the herbicide safener, fenclorim, among other compounds, and has been attributed to intra-vacuolar peptidases, which successively cleave the glycyl and glutamyl moieties from the attached glutathione (Figure 2B).^{21, 42} Although the mass fragments enabled us to classify these metabolites as glutathione and cysteine conjugates, the transformation pathways and ultimate molecular structures could not be definitively determined.

In addition to glutathione conjugation, detoxification of metabolites with sugar moieties is a common pathway in plants that occurs on aromatic hydroxyl or amino groups.^{20, 43–45} Conjugation proceeds without prior phase I functionalization (e.g., refs 20, 35, 39) or after a phase I reaction.²² Conjugation with sugars decreases toxicity of the compound and these phase II metabolites are likely intermediates to permanently bound residues.^{12, 45}

Glucosyltransferases in *Arabidopsis* also conjugate TNT reduction products, forming *C*-, *O*-, and *N*-glycosidic conjugates, and β -D-glucopyranosides are common hexose sugar stereoisomers utilized by plants to detoxify organic contaminants.^{20, 22}

Here, the neutral losses observed for both M524 and M568 indicate a glycosylated and further conjugated sugar. M568 has a neutral loss of 248, indicative of a malonylated hexose sugar (m/z 162+86).²⁰ Malonylation is known to signal vacuolar sequestration in *Arabidopsis*, and is commonly observed in plant metabolism of glycosyl-conjugates.^{20, 42} M524 has a neutral loss of 204, corresponding to a loss of acetyl-hexose (162+42) and contains the same aglycone moiety as M568. The mass difference between M568 and M524 (m/z 43.9875) is equivalent to CO₂ (m/z 43.9898). Abiotic decarboxylation of a malonyl-glycoside to yield the acetyl-glycoside has been observed for other *Arabidopsis* metabolites, which we believe to occur with M568, yielding M524 (Figure 2C).⁴²

To further investigate the identity of M330, we hydrolyzed plant extracts and analyzed the resulting solution by LC-QQQ. Under acidic conditions, a decrease of M330 was concomitant with an increase in 2-ANAN, further validating the structure of M330 as a hexose-conjugate of 2-ANAN (Figure S4). We quantified M330 redundantly using LC-QQQ peak area of M330 calibrated to 2-ANAN peak area and by measuring 2-ANAN resulting from acid hydrolysis of the plant extracts. The first method assumed that M330 and 2-ANAN had the same ionization efficiencies, and therefore detector response, per mole of mass. This assumption is supported by a study where acylated amines had an average mass spectrometer detector response factor of 1.5 times when compared to the unconjugated amine, providing an approximation of transformation product mass.⁴⁶ The second method quantified M330 as 2-ANAN assuming complete acid hydrolysis, no other loss of 2-ANAN, and no ion suppression in the mass spectrometer. The two methods similarly found that M330 made up 1.7% or 1.8% of the DNAN mass taken up after 3 days, respectively.

Glycosylated metabolites accumulate over three days—We measured each metabolite in whole plants and hydroponic media over three days of DNAN exposure. While ten phase II conjugates of DNAN were detected by LC-QToF and LC-Orbitrap, we were unable to detect some metabolites by LC-QQQ. In contrast, some glycosylated metabolites (M524, M568, and M330) accumulated over the 72-hour exposure. Similarly, a glycosylated metabolite accumulated over time when *Arabidopsis* metabolized benzotriazole and the metabolite was released into the media.³⁵ Here, little M330 accumulated in the media, but plant tissues contained M330 at levels comparable to DNAN and 2-ANAN. The mass balance after three days was low (i.e., 8% of DNAN taken up), suggesting that DNAN conjugates were sequestered into cell walls or vacuoles through phase III metabolism, similar to TNT in other plants.⁴⁷ For example, hybrid poplar trees sequestered about half of [¹⁴C]TNT to non-extractable residues, and 27% of ¹⁴C from [¹⁴C]TNT was covalently bound to lignin in wheat.^{11, 48} *Arabidopsis* also quickly and extensively metabolizes naproxen and diclofenac to non-extractable residues.^{49, 50} In addition to phase III metabolism, the low mass balance could be the result of unidentified and non-extractable bound residues, incorrect assumptions in the M330 mass approximation, low ionization efficiency of identified metabolites, or in-source fragmentation of identified or other non-identified conjugated metabolites.

[¹⁵N₂]DNAN and glycosylated [¹⁵N₂]DNAN metabolite are photolyzed in leaves to yield ¹⁵NO₂

To determine the potential for DNAN and DNAN metabolites to be photolyzed inside plants, we subjected *Arabidopsis* leaves to simulated sunlight after two days of exposure to [¹⁵N₂]DNAN in a growth chamber. The [¹⁵N₂]DNAN and [¹⁵N₂]M330 metabolite were significantly photolyzed compared to foil wrapped controls ($p < 0.001$ and $p = 0.005$, respectively, matched pairs Student's t-test for $n = 5$ triplicate pairs, Figure 4). The DNAN in the leaf fraction at the beginning of the simulated sunlight experiment was 0.7% of the total amount taken up by the plants after two days, which is 8.1% of the DNAN detected in the whole plants in the mass balance experiment. Other metabolites were not detected in the leaf fractions. Besides RDX photolysis in grass blades and poplar tissues, *in planta* photolysis has not been investigated for other compounds to our knowledge.^{24,25} In fact, a recent review of plant uptake of pharmaceuticals and personal care products stated “we are not aware of any studies confirming photodegradation of contaminants within plants.”²⁶ One recent study speculated that photolysis inside leaves could alter sulfamethoxazole concentrations in lettuce and strawberry shoots, but the effect was not investigated.⁵¹ Therefore, we believe this is the first demonstration of photolysis of a plant xenobiotic metabolite *in planta*.

DNAN is directly photolyzed in solution to yield nitrite and nitrate.³¹ Therefore, we measured ¹⁵NO₂ evolution in photolyzed leaves exposed to [¹⁵N₂]DNAN (Figure 5). The results clearly show that ¹⁵NO₂ is present in higher concentrations in light-exposed leaves than in dark controls ($p < 0.0001$, $n = 5$ triplicate pairs), albeit at low concentrations. The production of ¹⁵N-labeled nitrite indicates that [¹⁵N₂]DNAN, or its metabolites, are denitrated by light inside the plant leaves. The concentration of ¹⁵NO₂ corresponded well with the amount of [¹⁵N₂]DNAN that was degraded, reaching a maximum of 77% of the initial [¹⁵N₂]DNAN concentration in the leaf on a molar basis. Interestingly, this denitration process occurred abiotically, and we did not detect any plant metabolites with only one ¹⁵N label (Tables 1 and S4). Since nitro groups impart toxicity and stability through resonance, the observed denitration represents an important step towards detoxifying DNAN.⁹ Some photolysis of DNAN and its metabolites in the growth chamber is unavoidable, which likely why some ¹⁵NO₂ was detected in dark control leaves. However, there was not a significant difference in unlabeled NO₂ in the dark and light-exposed plants ($p = 0.81$), further confirming that the ¹⁵NO₂ resulted from labeled DNAN. The decrease in nitrite after two hours of photolysis is likely due to oxidation of nitrite to nitrate, observed during DNAN photolysis in aqueous solution, but we were not able to accurately quantify nitrate at these levels using a reduction step before derivitization.³¹ In addition to photo-oxidation, nitrite and nitrate could be incorporated into other plant molecules, contributing to the observed decrease in nitrite. Light-exposed leaves grouped differently than dark-control leaves in a principal components analysis (Figure S5), but additional photolysis products could not be identified by the untargeted metabolomics approach described above. Further studies would be required to identify the metabolite photo-products. Despite the observed photolysis of DNAN and M330, sudden exposure of the plant leaves to higher levels of UV may overestimate the level of DNAN photolysis occurring in the field. Plants can adapt to higher levels of UV radiation by producing carotenoids to attenuate some UV excitation, and

sudden oxidative stress response could alter the transformation of the compounds as well.
52, 53

Environmental Implications—Knowledge of DNAN plant uptake and transformation products will inform phytoremediation feasibility assessments for DNAN-contaminated sites. Our work, and the work of others, showed plants take up DNAN from contaminated soil and water, but further work with field-relevant species are required to confirm the benefits of DNAN phytoremediation.^{1, 33} Beyond phytoremediation, plants can also be used as inexpensive sensors to monitor contaminant presence and concentration gradients without costly and invasive sampling techniques.^{54–57} Our work suggests that measuring 2-ANAN or DNAN inside plant tissues would under-predict actual DNAN uptake and metabolism, making correlations to porewater DNAN concentration problematic without further investigation and result in conservative estimates of phytoremediation efficacy. Our discovery of photo-denitration of DNAN indicates that photolysis may be an overlooked mechanism for transforming and detoxifying contaminants taken up by plants under field conditions. Although a minor proportion of the DNAN was transformed *via* this pathway, the mechanism could be more important for non-metabolized compounds or photoactive metabolites that would otherwise be shielded from sunlight in soil or porewater.

Supporting Information—Recipe for MS basal medium, additional liquid chromatography-mass spectrometry parameters, chemicals and reagents, XCMS (metabolomics) parameters, stable-isotope labeled metabolite summary tables, solar simulator irradiance spectra, uptake kinetics at higher initial concentrations, phase I metabolite concentrations in plant tissues and media, chromatograms of M330 hydrolysis, and principal components plot of photolyzed leaves.

Supplementary Material

Refer to Web version on PubMed Central for supplementary material.

Acknowledgments

The authors would like to thank Kaitlyn Drees for assistance with laboratory work. We also thank Stephen Harvey at the University of Minnesota Center for Mass Spectrometry and Proteomics for Orbitrap analysis. Funding for H.W.S. was from a National Science Foundation Graduate Research Fellowship (#000390183) and a University of Iowa Presidential Graduate Research Fellowship. Synthesis of the isotope-labeled DNAN was supported by a pilot grant from the University of Iowa Water Sustainability Initiative Iowa and the Iowa Superfund Research Program (P42 ES013661) funded by the National Institute of Environmental Health Sciences, National Institutes of Health.

References

1. Dodard SG, Sarrazin M, Hawari J, Paquet L, Ampleman G, Thiboutot S, Sunahara GI. Ecotoxicological assessment of a high energetic and insensitive munitions compound: 2,4-Dinitroanisole (DNAN). *J Hazard Mater.* 2013; 262:143–150. [PubMed: 24021166]
2. Pichtel J. Distribution and Fate of Military Explosives and Propellants in Soil: A Review. *Appl Environ Soil Sci.* 2012; 2012
3. Hawari J, Monteil-Rivera F, Perreault NN, Halasz A, Paquet L, Radovic-Hrapovic Z, Deschamps S, Thiboutot S, Ampleman G. Environmental fate of 2,4-dinitroanisole (DNAN) and its reduced products. *Chemosphere.* 2014; 119:16–23. [PubMed: 25460743]

4. Taylor S, Park E, Bullion K, Dontsova K. Dissolution of three insensitive munitions formulations. *Chemosphere*. 2015; 119:342–348. [PubMed: 25043961]
5. Boddu VM, Abburi K, Maloney SW, Damavarapu R. Thermophysical properties of an insensitive munitions compound, 2,4-dinitroanisole. *J Chem Eng Data*. 2008; 53(5):1120–1125.
6. Ro KS, Venugopal A, Adrian DD, Constant D, Qaisi K, Valsaraj KT, Thibodeaux LJ, Roy D. Solubility of 2,4,6-trinitrotoluene (TNT) in water. *J Chem Eng Data*. 1996; 41(4):758–761.
7. Fung, V., Schreiber, B., Patel, C., Samuels, P., Vinh, P., Zhao, X-L. Process Improvement and Optimization of Insensitive Explosive IMX-101. *Insensitive Munitions & Energetic Material Technology Symposium*; Las Vegas, NV. 2012. <https://ndiastorage.blob.core.usgovcloudapi.net/ndia/2012/IMEM/13862fung8B.pdf>
8. Hannink NK, Rosser SJ, Bruce NC. Phytoremediation of explosives. *Crit Rev Plant Sci*. 2002; 21(5):511–538.
9. Gunning V, Tzafestas K, Sparrow H, Johnston EJ, Brentnall AS, Potts JR, Rylott EL, Bruce NC. *Arabidopsis* glutathione transferases U24 and U25 exhibit a range of detoxification activities with the environmental pollutant and explosive, 2,4,6-trinitrotoluene. *Plant Physiol*. 2014; 165:854–865. [PubMed: 24733884]
10. Thompson PL, Ramer LA, Schnoor JL. Hexahydro-1,3,5-trinitro-1,3,5-triazine translocation in poplar trees. *Environ Toxicol Chem*. 1999; 18(2):279–284.
11. Thompson PL, Ramer LA, Schnoor JL. Uptake and transformation of TNT by hybrid poplar trees. *Environ Sci Technol*. 1998; 32(7):975–980.
12. Bhadra R, Wayment DG, Hughes JB, Shanks JV. Confirmation of conjugation processes during TNT metabolism by axenic plant roots. *Environ Sci Technol*. 1999; 33(3):446–452.
13. Hughes JB, Shanks J, Vanderford M, Lauritzen J, Bhadra R. Transformation of TNT by aquatic plants and plant tissue cultures. *Environ Sci Technol*. 1997; 31(1):266–271.
14. Rylott EL, Jackson RG, Edwards J, Womack GL, Seth-Smith HMB, Rathbone DA, Strand SE, Bruce NC. An explosive-degrading cytochrome P450 activity and its targeted application for the phytoremediation of RDX. *Nat Biotech*. 2006; 24(2):216–219.
15. Sheremata TW, Hawari J. Mineralization of RDX by the white rot fungus *Phanerochaete chrysosporium* to carbon dioxide and nitrous oxide. *Environ Sci Technol*. 2000; 34(16):3384–3388.
16. Fernando T, Bumpus JA, Aust SD. Biodegradation of TNT (2,4,6-trinitrotoluene) by *Phanerochaete chrysosporium*. *Appl Environ Microbiol*. 1990; 56(6):1666–1671. [PubMed: 2383008]
17. Hughes JB, Wang C, Yesland K, Richardson A, Bhadra R, Bennett G, Rudolph F. Bamberger rearrangement during TNT metabolism by *Clostridium acetobutylicum*. *Environ Sci Technol*. 1998; 32(4):494–500.
18. Hawari J, Halasz A, Groom C, Deschamps S, Paquet L, Beaulieu C, Corriveau A. Photodegradation of RDX in aqueous solution: a mechanistic probe for biodegradation with *Rhodococcus* sp. *Environ Sci Technol*. 2002; 36(23):5117–5123. [PubMed: 12523428]
19. Sandermann H. Plant metabolism of xenobiotics. *Trends Biochem Sci*. 1992; 17(2):82–84. [PubMed: 1566333]
20. Macherius A, Eggen T, Lorenz W, Moeder M, Ondruschka J, Reemtsma T. Metabolization of the bacteriostatic agent triclosan in edible plants and its consequences for plant uptake assessment. *Environ Sci Technol*. 2012; 46(19):10797–10804. [PubMed: 22989227]
21. Coleman J, Blake-Kalff M, Davies E. Detoxification of xenobiotics by plants: chemical modification and vacuolar compartmentation. *Trends in Plant Sci*. 1997; 2(4):144–151.
22. Gandia-Herrero F, Lorenz A, Larson T, Graham IA, Bowles DJ, Rylott EL, Bruce NC. Detoxification of the explosive 2,4,6-trinitrotoluene in *Arabidopsis*: discovery of bifunctional O- and C-glucosyltransferases. *The Plant Journal*. 2008; 56(6):963–974. [PubMed: 18702669]
23. Durringer JM, Morrie Craig A, Smith DJ, Chaney RL. Uptake and transformation of soil [¹⁴C]-trinitrotoluene by cool-season grasses. *Environ Sci Technol*. 2010; 44(16):6325–6330. [PubMed: 20666491]
24. Just CL, Schnoor JL. Phytodegradation of hexahydro-1,3,5-trinitro-1,3,5-triazine (RDX) in leaves of reed canary grass. *Environ Sci Technol*. 2004; 38(1):290–295. [PubMed: 14740749]

25. Van Aken B, Yoon JM, Just CL, Schnoor JL. Metabolism and mineralization of hexahydro-1,3,5-trinitro-1,3,5-triazine inside poplar tissues (*Populus deltoides* × *nigra* DN-34). *Environ Sci Technol*. 2004; 38(17):4572–4579. [PubMed: 15461165]
26. Müller EL, Nason SL, Karthikeyan KG, Pedersen JA. Root uptake of pharmaceuticals and personal care product ingredients. *Environ Sci Technol*. 2016; 50(2):525–541. [PubMed: 26619126]
27. Olivares C, Liang J, Abrell L, Sierra-Alvarez R, Field JA. Pathways of reductive 2,4-dinitroanisole (DNAN) biotransformation in sludge. *Biotechnol Bioeng*. 2013; 110(6):1595–1604. [PubMed: 23280483]
28. Olivares CI, Abrell L, Khatiwada R, Chorover J, Sierra-Alvarez R, Field JA. (Bio)transformation of 2, 4-dinitroanisole (DNAN) in soils. *J Hazard Mater*. 2016; 304:214–221. [PubMed: 26551225]
29. Schroer HW, Langenfeld KL, Li X, Lehmler H-J, Just CL. Stable isotope-enabled pathway elucidation of 2,4-dinitroanisole metabolized by *Rhizobium litchii*. *Environ Sci Technol Lett*. 2015; 2(12):362–366.
30. Olivares CI, Sierra-Alvarez R, Alvarez-Nieto C, Abrell L, Chorover J, Field JA. Microbial toxicity and characterization of DNAN (bio)transformation product mixtures. *Chemosphere*. 2016; 154:499–506. [PubMed: 27085064]
31. Rao B, Wang W, Cai Q, Anderson T, Gu B. Photochemical transformation of the insensitive munitions compound 2,4-dinitroanisole. *Sci Total Environ*. 2013; 443:692–699. [PubMed: 23228715]
32. Schroer HW, Langenfeld KL, Li X, Lehmler H-J, Just CL. Biotransformation of 2,4-dinitroanisole by a fungal *Penicillium* sp. *Biodegradation*. 2017; 28(1):95–109. [PubMed: 27913891]
33. Richard T, Weidhaas J. Dissolution, sorption, and phytoremediation of IMX-101 explosive formulation constituents: 2,4-dinitroanisole (DNAN), 3-nitro-1,2,4-triazol-5-one (NTO), and nitroguanidine. *J Hazard Mater*. 2014; 280:561–569. [PubMed: 25212590]
34. Yamada T, Sawada M, Taki M. Photolysis of aryl glycosides with ultraviolet irradiation. *Agric Biol Chem*. 1975; 39:909–910.
35. LeFevre GH, Müller CE, Li RJ, Luthy RG, Sattely ES. Rapid phytotransformation of benzotriazole generates synthetic tryptophan and auxin analogs in *Arabidopsis*. *Environ Sci Technol*. 2015; 49(18):10959–10968. [PubMed: 26301449]
36. LeFevre GH, Portmann AC, Müller CE, Sattely ES, Luthy RG. Plant assimilation kinetics and metabolism of 2-mercaptobenzothiazole tire rubber vulcanizers by *Arabidopsis*. *Environ Sci Technol*. 2016; 50(13):6762–6771. [PubMed: 26698834]
37. Nussler AK, Glanemann M, Schirmeier A, Liu L, Nussler NC. Fluorometric measurement of nitrite/nitrate by 2,3-diaminonaphthalene. *Nat Protocols*. 2006; 1(5):2223–2226. [PubMed: 17406460]
38. Gowda H, Ivanisevic J, Johnson CH, Kurczyk ME, Benton HP, Rinehart D, Nguyen T, Ray J, Kuehl J, Arevalo B, Westenskow PD, Wang J, Arkin AP, Deutschbauer AM, Patti GJ, Siuzdak G. Interactive XCMS online: simplifying advanced metabolomic data processing and subsequent statistical analyses. *Anal Chem*. 2014; 86(14):6931–6939. [PubMed: 24934772]
39. Macherius A, Seiwert B, Schröder P, Huber C, Lorenz W, Reemtsma T. Identification of plant metabolites of environmental contaminants by UPLC-QToF-MS: The *in vitro* metabolism of triclosan in horseradish. *J Agric Food Chem*. 2014; 62(5):1001–1009. [PubMed: 24456336]
40. Schymanski EL, Jeon J, Gulde R, Fenner K, Ruff M, Singer HP, Hollender J. Identifying small molecules via high resolution mass spectrometry: communicating confidence. *Environ Sci Technol*. 2014; 48(4):2097–2098. [PubMed: 24476540]
41. Xie C, Zhong D, Chen X. A fragmentation-based method for the differentiation of glutathione conjugates by high-resolution mass spectrometry with electrospray ionization. *Anal Chim Acta*. 2013; 788:89–98. [PubMed: 23845486]
42. Brazier-Hicks M, Evans KM, Cunningham OD, Hodgson DRW, Steel PG, Edwards R. Catabolism of glutathione conjugates in *Arabidopsis thaliana*: role in metabolic reactivation of the herbicide safener fenclorim. *J Biol Chem*. 2008; 283(30):21102–21112. [PubMed: 18522943]
43. Colby SR. Herbicide metabolism: *N*-glycoside of amiben isolated from soybean plants. *Science*. 1965; 150(3696):619–620. [PubMed: 5891144]

44. Winkler R, Sandermann H. *N*-Glucosyl conjugates of chlorinated anilines: spontaneous formation and cleavage. *J Agric Food Chem.* 1992; 40(10):2008–2012.
45. McCutcheon, SC., Schnoor, JL., editors. *Phytoremediation: transformation and control of contaminants.* John Wiley & Sons, Inc; Hoboken, New Jersey: 2003.
46. Gulde R, Meier U, Schymanski EL, Kohler H-PE, Helbling DE, Derrer S, Rentsch D, Fenner K. Systematic exploration of biotransformation reactions of amine-containing micropollutants in activated sludge. *Environ Sci Technol.* 2016; 50(6):2908–2920. [PubMed: 26864277]
47. Sandermann H. Higher plant metabolism of xenobiotics: the 'green liver' concept. *Pharmacogenetics.* 1994; 4(5):225–241. [PubMed: 7894495]
48. Sens C, Scheidemann P, Werner D. The distribution of ¹⁴C-TNT in different biochemical compartments of the monocotyledonous *Triticum aestivum*. *Environ Pollut.* 1999; 104(1):113–119.
49. Fu Q, Zhang J, Borchardt D, Schlenk D, Gan J. Direct conjugation of emerging contaminants in *Arabidopsis*: indication for an overlooked risk in plants? *Environ Sci Technol.* 2017; 51(11):6071–6081. [PubMed: 28502169]
50. Fu Q, Ye Q, Zhang J, Richards J, Borchardt D, Gan J. Diclofenac in *Arabidopsis* cells: Rapid formation of conjugates. *Environmental Pollution.* 2017; 222(Supplement C):383–392. [PubMed: 28012668]
51. Hyland KC, Blaine AC, Higgins CP. Accumulation of contaminants of emerging concern in food crops—part 2: plant distribution. *Environ Toxicol Chem.* 2016; 34(10):2222–2230.
52. Holt NE, Zigmantas D, Valkunas L, Li X-P, Niyogi KK, Fleming GR. Carotenoid cation formation and the regulation of photosynthetic light harvesting. *Science.* 2005; 307(5708):433. [PubMed: 15662017]
53. Ramel F, Birtic S, Ginies C, Soubigou-Taconnat L, Triantaphylidès C, Havaux M. Carotenoid oxidation products are stress signals that mediate gene responses to singlet oxygen in plants. *Proc Natl Acad Sci.* 2012; 109(14):5535–5540. [PubMed: 22431637]
54. Limmer MA, Balouet J-C, Karg F, Vroblesky DA, Burken JG. Phytoscreening for chlorinated solvents using rapid in vitro SPME sampling: application to urban plume in Verl, Germany. *Environ Sci Technol.* 2011; 45(19):8276–8282. [PubMed: 21848303]
55. Limmer MA, Shetty MK, Markus S, Kroeker R, Parker BL, Martinez C, Burken JG. Directional phytoscreening: contaminant gradients in trees for plume delineation. *Environ Sci Technol.* 2013; 47(16):9069–9076. [PubMed: 23937095]
56. Limmer MA, Holmes AJ, Burken JG. Phytomonitoring of chlorinated ethenes in trees: a four-year study of seasonal chemodynamics *in planta*. *Environ Sci Technol.* 2014; 48(18):10634–10640. [PubMed: 25140854]
57. Limmer MA, West DM, Mu R, Shi H, Whitlock K, Burken JG. Phytoscreening for perchlorate: rapid analysis of tree sap. *Environ Sci: Water Res Technol.* 2015; 1(2):138–145.

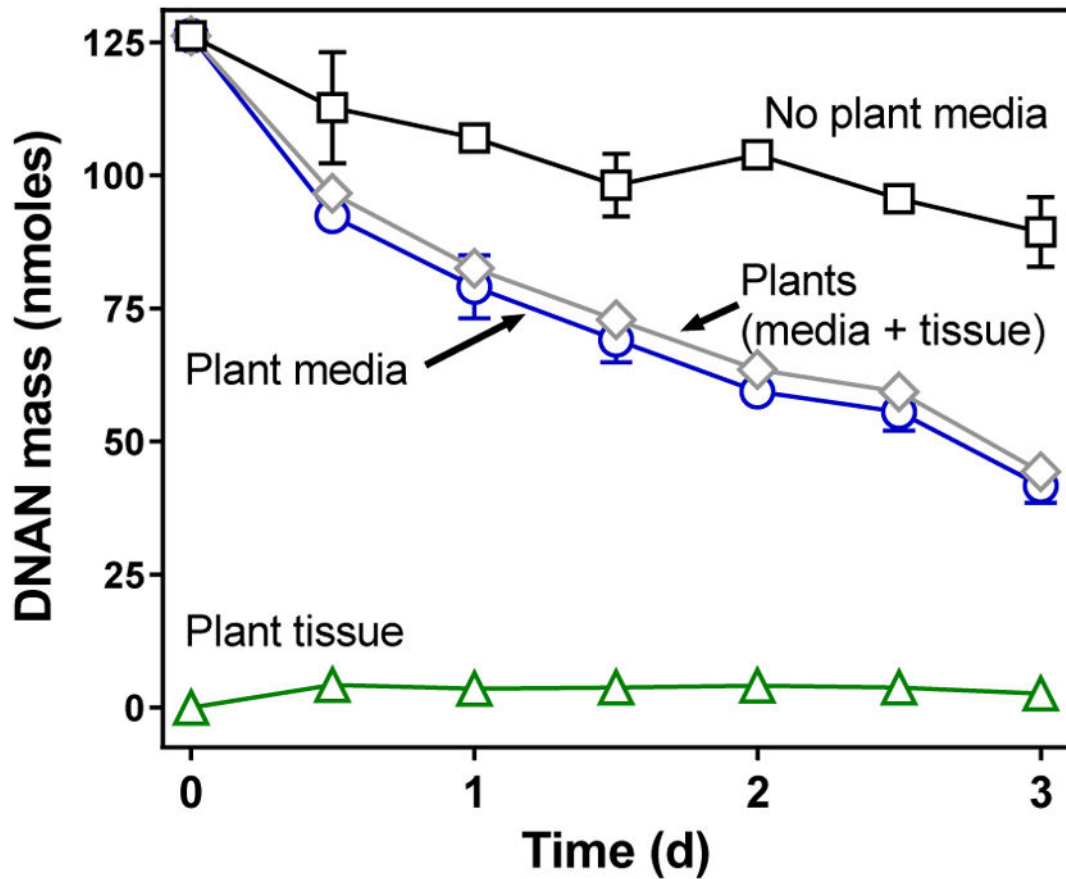


Figure 1. DNAN mass in hydroponic media and *Arabidopsis* whole plant tissue as a function of time. Error bars are \pm standard error of the mean ($n = 3$ plant tissue and media, $n = 2$ media, no plant control) and are not displayed when within the markers.

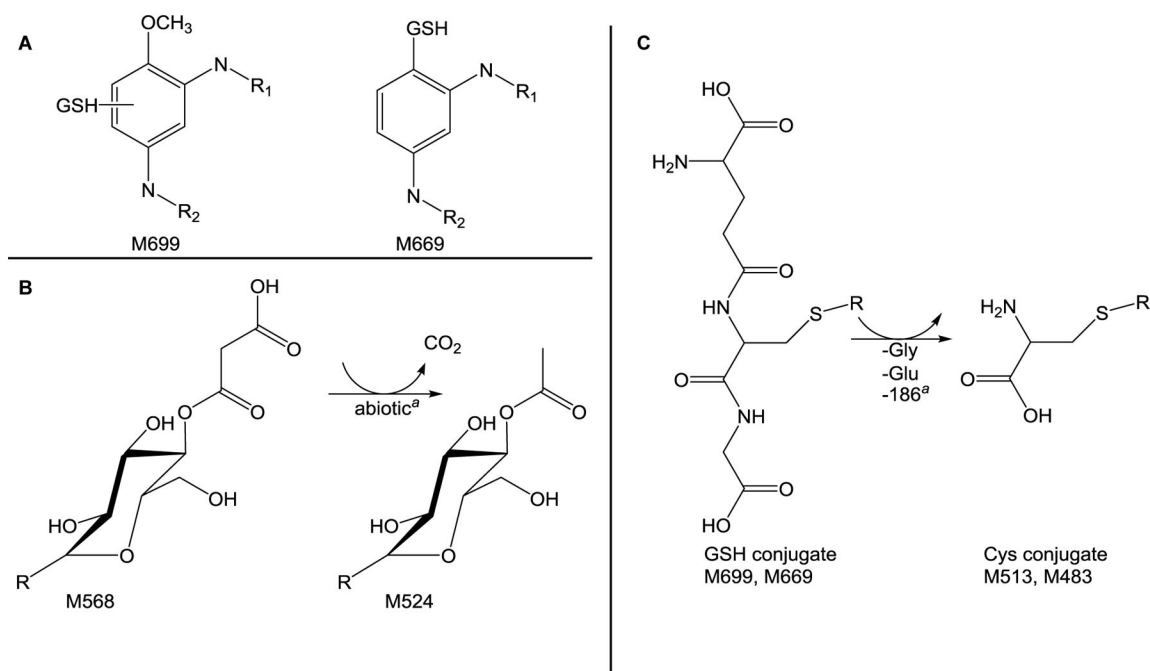


Figure 2. Proposed relationships between some identified DNAN metabolites in *Arabidopsis*. A) Proposed glutathione conjugation B) abiotic decarboxylation of M568 to yield M524 C) glutathione degradation to cysteinyl metabolites. Abbreviations: GSH (glutathione), Cys (cysteine), R (unknown moiety). ^aref. 42.

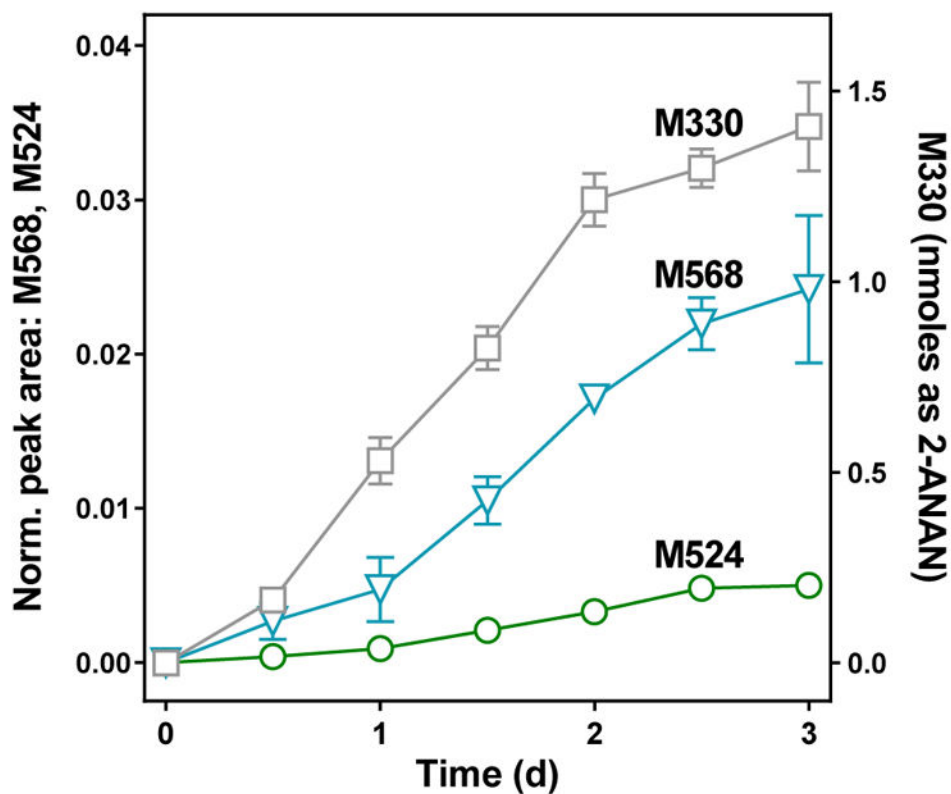


Figure 3. Metabolite formation over time in whole plant tissues. M568 and M524 are expressed as LC-QQQ peak area of metabolite normalized to internal standard [$^{13}\text{C}_6$]DNAN and dry weight of plant material (mg). M330 is quantified as peak area quantified with a 2-ANAN calibration curve. Error bars are \pm standard error of the mean ($n = 3$) and are not displayed when within the markers.

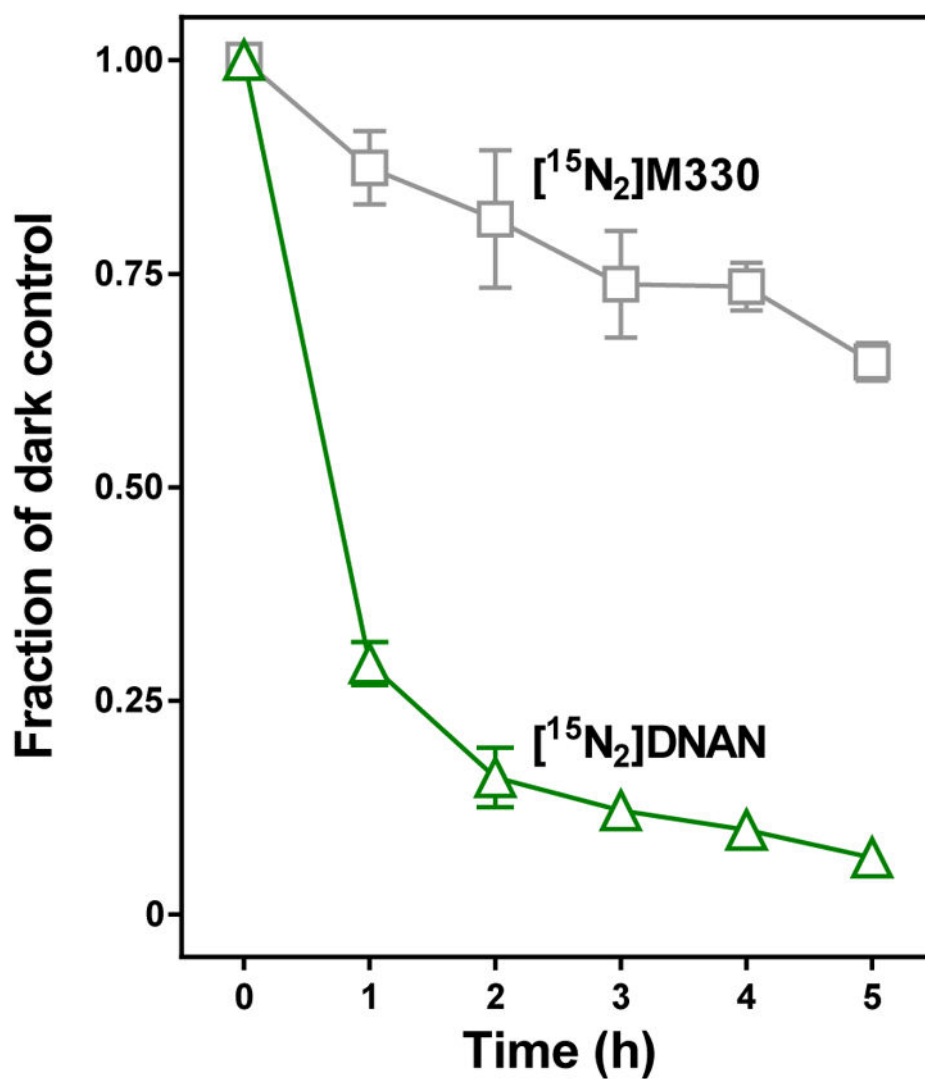


Figure 4. DNAN and M330 in *Arabidopsis* leaves during exposure to simulated sunlight (20 °C, 750 W/m²). Data are LC-QQQ peak area of compounds in light-exposed leaf extracts normalized to foil-wrapped, dark control extracts and dry weight. Error bars are ± standard error of the mean (n = 3) and are not displayed when within the markers.

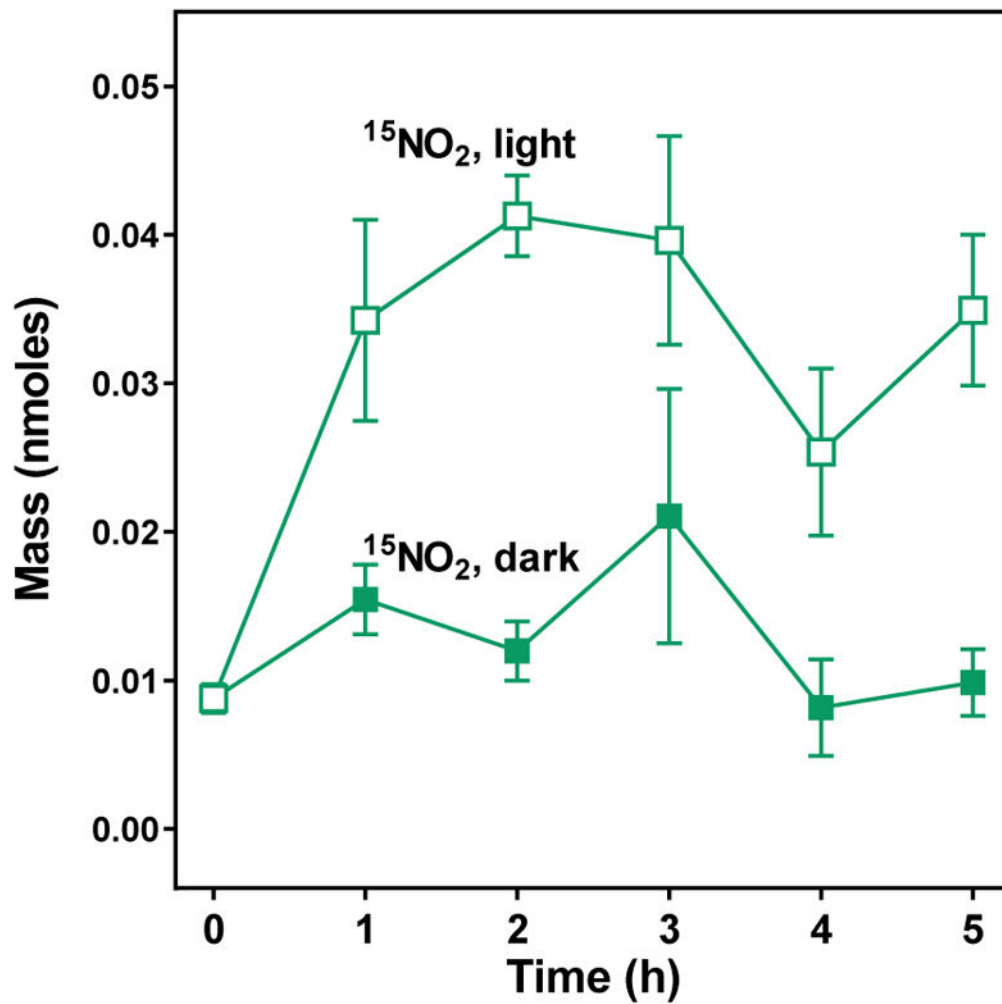
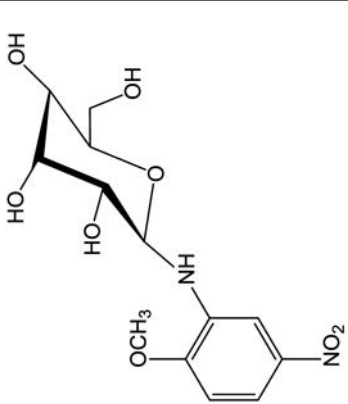
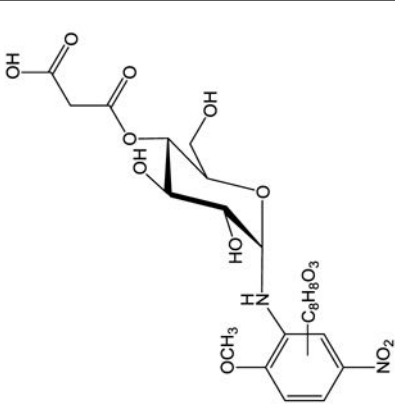
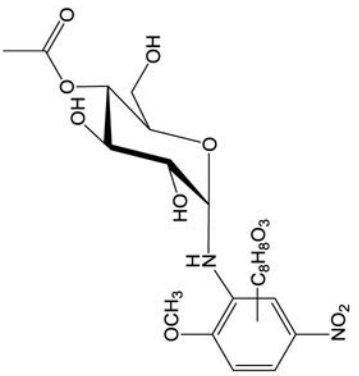
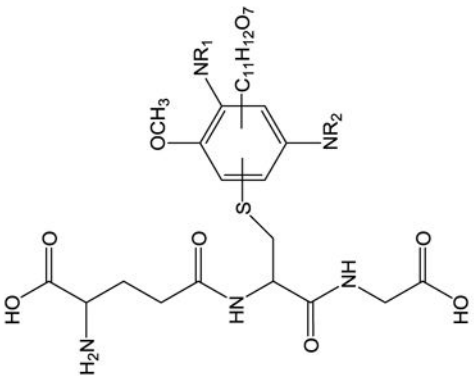


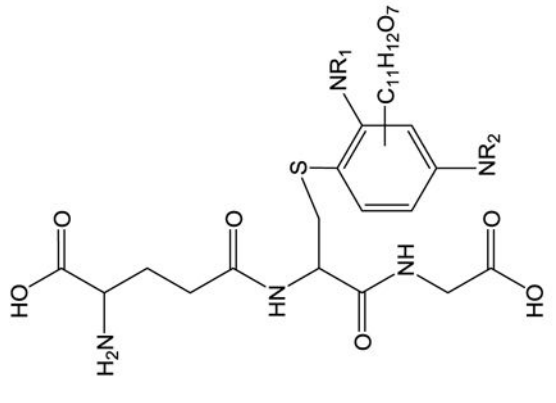
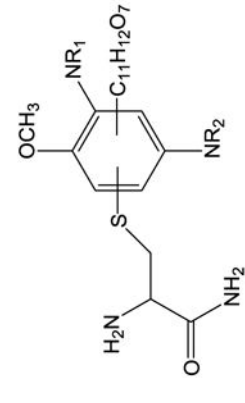
Figure 5. ¹⁵NO₂ measured in leaf extracts exposed to simulated sunlight or in the dark. Error bars are \pm standard error of the mean (n = 3).

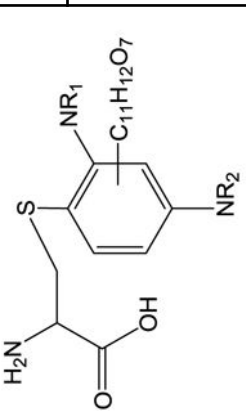
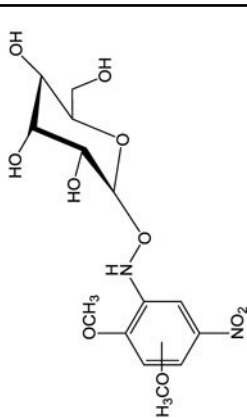
Table 1

Summary of phase II DNAN metabolites identified in *Arabidopsis* plant tissue after 48 hours of exposure.

| metabolite | proposed structure ^a | confidence level ^b | RT (min) | proposed ion | proposed ion formula | accurate mass | deviation mDa (ppm) | fragments (nominal m/z) |
|------------|--|-------------------------------|----------|--------------------|--|---------------|---------------------|--------------------------|
| M330 |  | 2 | 3.4 | [M+H] ⁺ | C ₁₃ H ₁₉ N ₂ O ₈ | 331.1129 | 1.3 (3.8) | 169 |
| M568 |  | 3 | 4.4 | [M+H] ⁺ | C ₂₄ H ₂₉ N ₂ O ₁₄ | 569.1604 | 1.5 (2.6) | 321 304 289 274 |

| metabolite | proposed structure ^a | confidence level ^b | RT (min) | proposed ion | proposed ion formula | accurate mass | deviation mDa (ppm) | fragments (nominal m/z) |
|------------|--|-------------------------------|----------|--------------------|--|---------------|---------------------|--|
| M524 |  | 3 | 3.9 | [M-H] ⁻ | C ₂₃ H ₂₇ N ₃ O ₁₂ | 523.1573 | 0.9 (1.7) | 319 303 289 152 |
| M699 |  | 3 | 3.0 | [M+H] ⁺ | C ₂₈ H ₃₈ N ₅ O ₁₄ S | 700.2117 | -0.6 (0.9) | 393 308 274 130 306 272 143 128 |
| | | | | [M-H] ⁻ | C ₂₈ H ₃₆ N ₅ O ₁₄ S | 698.1992 | -1.3 (1.8) | |

| metabolite | proposed structure ^a | confidence level ^b | RT (min) | proposed ion | proposed ion formula | accurate mass | deviation mDa (ppm) | fragments (nominal m/z) |
|------------|--|-------------------------------|----------|--------------------|--|---------------|---------------------|--|
| M669 |  | 3 | 3.1 | [M+H] ⁺ | C ₂₇ H ₃₆ N ₅ O ₁₃ S | 670.2013 | 1.7 (2.6) | 363 308 145 130 306 272 143 128 |
| | | | | [M-H] ⁻ | C ₂₇ H ₃₄ N ₅ O ₁₃ S | 668.1886 | 1.2 (1.8) | |
| M513 |  | 4 | 3.4 | [M+H] ⁺ | C ₂₁ H ₂₈ N ₃ O ₁₀ S | 514.1484 | 1.1 (2.2) | N/A |
| | | | | [M-H] ⁻ | C ₂₁ H ₂₆ N ₃ O ₁₀ S | 512.1347 | 0.8 (1.6) | |

| metabolite | proposed structure ^a | confidence level ^b | RT (min) | proposed ion | proposed ion formula | accurate mass | deviation mDa (ppm) | fragments (nominal m/z) |
|------------|---|-------------------------------|----------|--------------------|---|---------------|---------------------|-------------------------|
| M483a |  | 4 | 3.4 | [M+H] ⁺ | C ₂₀ H ₂₆ N ₃ O ₉ S | 484.1379 | 1.1 (2.2) | N/A |
| M483b | | 4 | 3.5 | [M-H] ⁻ | C ₂₀ H ₂₄ N ₃ O ₉ S | 482.1244 | 1.1 (2.2) | N/A |
| M376 |  | 4 | 2.4 | [M-H] ⁻ | C ₁₄ H ₁₉ N ₂ O ₁₀ | 375.1041 | -0.1 (0.4) | N/A |
| M808 | | 5 | 2.4 | N/A | N/A | 807.1708 | N/A | N/A |

^aR₁ and R₂ are H₂ in these structural approximations, and β-D-glucopyranoside is presented as the conjugated hexose sugar moiety. These structures represent the potential variety of nitro-reduction states, hexose sugars, and conjugation locations (i.e., positional isomers) that cannot be determined by mass spectrometry alone.

^bconfidence was assigned using the Schymanski, et al. framework, briefly, 2: probable structure, 3: tentative candidate, 4: unequivocal molecular formula, 5: exact mass only.⁴⁰